https://doi.org/10.5194/tc-2019-302
Preprint. Discussion started: 4 February 2020


The Cryosphere Discussions
Open Access
EGU

# How much snow falls in the world's mountains? A first look at mountain snowfall estimates in A-train observations and reanalyses.

Anne Sophie Daloz[1,2,3], Marian Mateling[4], Tristan L'Ecuyer[2,4], Mark Kulie[5], Norm B. Wood[1], Mikael Durand[6], Melissa Wrzesien[7], Camilla W. Stjern[3] and Ashok P. Dimri[8].

1. Space Science and Engineering Center (SSEC), University of Wisconsin-Madison, 1225 West Dayton Street, 53706 Madison, WI, USA
2. Center for Climatic Research (CCR), University of Wisconsin-Madison, 1225 West Dayton Street, 53706 Madison, WI, USA
3. Center for International Climate Research (CICERO) Gaustadalleen 21, 0349, Oslo, Norway
4. Department of Atmospheric and Oceanic Sciences (AOS), University of Wisconsin-Madison 1225 West Dayton Street, 53706 Madison, WI, USA
5. NOAA/NESDIS/STAR/Advanced Satellite Products Branch 1225 West Dayton Street, Madison, WI 53706, USA
6. School of Earth Sciences and Byrd Polar and Climate Research Center, Ohio State University 108 Scott Hall, 1090 Carmack Rd, Columbus OH, 43210, USA
7. Department of Geological Sciences, University of North Carolina at Chapel Hill Chapel Hill, NC 25799, USA
8. School of Environmental Sciences, Jawaharlal Nehru University, New Delhi, 110067, India

*Correspondence to:* Anne Sophie Daloz (anne.sophie.daloz@cicero.oslo.no)

https://doi.org/10.5194/tc-2019-302
Preprint. Discussion started: 4 February 2020


The Cryosphere Discussions
Open Access
EGU

**Abstract**

CloudSat estimates that 1773 cubic km of snow falls, on average, each year over the world's mountains. This volume of snow amounts to five percent of the volume of snowfall accumulations globally. This study provides a synthesis of mountain snowfall estimates over the four continents containing mountains (Eurasia, North America, South America and Africa), comparing snowfall estimates from a new observation-based dataset to similar snowfall estimates from four reanalyses: Modern-Era Retrospective analysis for Research and Applications (MERRA), MERRA-2, Japanese 55-year Reanalysis (JRA-55) and European Center for Medium-Range Weather Forecasts Re-Analysis (ERA-Interim). Globally, the fraction of snow that falls in the world's mountains is very similar between all these independent datasets (4-5%), providing confidence in this estimate. The fraction of mountain snowfall for the different continents is also very similar between the different datasets. However, the magnitude of snowfall estimates differs substantially globally and for each continent. The consensus in fractions and the dissimilarities in magnitude could indicate that large-scale forcings are similarly represented in the five datasets while at smaller scales there might be large discrepancies.

https://doi.org/10.5194/tc-2019-302
Preprint. Discussion started: 4 February 2020


52 **1. Introduction**

53 The advent of satellite-borne instruments capable of detecting falling snow and of reanalysis products that
54 diagnose snowfall have made possible a global examination of how snowfall is distributed and its contribution to
55 atmospheric and surface processes. Falling snow transfers moisture and latent energy between the atmosphere and
56 the surface. Snow impacts the surface radiant energy transfer by modifying albedo and emissivity. Accumulated
57 snow can also act as a thermal insulator that modifies sensible heat fluxes and how the response of surface
58 temperature responds to changes in atmospheric conditions. Furthermore, it acts as a surface water storage reservoir
59 (Rodell et al., 2018), providing seasonal runoff that provides fresh water supplies for both human populations and
60 water-dependent ecosystems. Billions of people around the world depends on these resources. These water supplies
61 are recognized as being at risk from climate change and rising global temperatures (Barnett et al., 2005; Mankin et
62 al., 2015).
63
64 Precipitation gauge measurements of snowfall for meteorological and hydrological purposes provide valuable
65 data but have historically suffered shortcomings related to spatial sampling and gauge performance (Kidd et al., 2017).
66 Shortcomings in the accuracy of such measurements and methods to improve that accuracy have been the focus of a
67 number of studies (Goodison et al., 1998; Kochendorfer et al., 2018). Beyond accuracy issues, these gauge networks
68 are necessarily of limited spatial coverage potentially biasing climatologies over large domains. Coverage of ocean
69 regions is not possible. Over land, gauges tend to be located near inhabited areas, leading to spare or nonexistent
70 coverage in more remote locations (Groisman and Legates, 1994). These remote locations include areas such as the
71 high latitudes and mountains, where snowfall can be the dominant form of precipitation. Even when these areas have
72 relatively dense gauge networks such as the CONUS (Contiguous United States) mountains, gridded datasets have
73 their limitations, most notably gauge under catchment issues and large snowfall accumulation gradients in complex
74 terrain that are often insufficiently sampled by existing in situ networks (Henn et al., 2018).
75
76 Given these shortcomings in snowfall surface observations, studies on snowfall in remote locations commonly
77 rely on reanalyses (e.g. Bromwich et al., 2011). Reanalyses utilize numerical weather prediction models to integrate
78 observations of large-scale geophysical fields (e.g., temperature and water vapor). One strength of reanalysis datasets
79 is their continuous spatial and temporal coverage. However, the veracity of reanalysis snowfall datasets depends

https://doi.org/10.5194/tc-2019-302
Preprint. Discussion started: 4 February 2020


80 strongly on the underlying model and the assimilated datasets, which often exhibit systematic and varied biases (Daloz
81 et al. 2018). In addition, their low spatial resolutions can be a limitation especially in regions of complex topography
82 and reanalyses should therefore be used with caution. For example, Wrzesien et al. (2019) showed that reanalyses
83 have large biases in terms of snow water equivalent (SWE) over North America but their representation of snowfall
84 is more realistic. In this current study, four reanalysis datasets will be examined: Modern-Era Retrospective analysis
85 for Research and Applications (MERRA), MERRA-2, European Centre for Medium-Range Weather Forecasts
86 (ECMWF) interim reanalysis (ERA-Interim) and Japanese 55-year Reanalysis (JRA-55).
87
88 As an alternative to reanalyses, snowfall rates can now be assessed using satellite observations (with sufficient
89 spatio-temporal coverage) provided by CloudSat's Cloud Profiling Radar (CPR). CloudSat observations, nearly
90 continuous since 2006 (Stephens et al., 2002, 2008), have been applied to produce near-global estimates of snowfall
91 occurrence and intensity (Liu 2008; Kulie and Bennartz, 2009; Wood and L'Ecuyer, 2018). The resulting datasets have
92 been examined extensively from local to global scales (Liu 2008; Kulie and Bennartz, 2009; Hiley et al., 2011; Palerme
93 et al., 2014; Smalley et al., 2015; Chen et al., 2016; Behrangi et al., 2016; Norin et al., 2015; Milani et al., 2018).
94 CloudSat has substantially extended the spatial extent of precipitation measurements compared to existing gauge or
95 radar networks. In particular, these instruments have greatly enhanced the observations of light precipitation including
96 snowfall over oceans, over remote high latitude regions and over inaccessible land areas (e.g., Behrangi et al., 2016;
97 Milani et al., 2018; Smalley et al., 2015; Norin et al., 2017).
98
99 However, satellite-based retrievals also have inherent uncertainties related, for example, to their limited
100 temporal coverage. For instance, they might miss some heavy events such as atmospheric rivers in Western North and
101 South America (Ralph et al., 2005; Neiman et al., 2008; Viale and Nunez, 2011). Therefore CloudSat snowfall
102 retrievals have been extensively assessed against a wide range of independent ground-based measurements. Hiley et
103 al. (2011) seasonally compared CloudSat snowfall estimates with Canadian surface gauge measurements, showing
104 better results for higher versus lower latitudes - especially lower latitude coastal sites. They speculated that latitudinal
105 comparison differences might be due to CloudSat sampling (more observations at higher latitudes), snow
106 microphysical differences associated with warmer snow events that could affect CloudSat estimates (e.g., wetter snow,
107 rimed snow, and/or mixed phase precipitation), or precipitation phase identification issues associated with snow events

https://doi.org/10.5194/tc-2019-302
Preprint. Discussion started: 4 February 2020


in the 0-4C temperature range. CloudSat's 2C-SNOW-PROFILE (2CSP) product also displayed excellent light snowfall detection capabilities when compared against the National Multi-Sensor Mosaic QPE System (NMQ) dataset, a hydrometeorological platform, which assimilates different observational network, but CloudSat did not produce higher snowfall rates as frequently as NMQ (Cao et al., 2014). Further comparisons between CloudSat and the National Centers for Environmental Prediction (NCEP) merged NEXRAD and rain gauge Stage IV dataset illustrated consistent CloudSat-Stage IV performance when near-surface temperatures are below freezing (Smalley et al., 2014). The CloudSat 2CSP product was also compared to a ground-based radar network in Sweden, showing consistent agreement in the 0.1 – 1.0 mm $h^{-1}$ snowfall rate range (Norin et al., 2015). However, 2CSP snowfall rate counts were lower above the 1 mm $h^{-1}$ threshold. 2CSP retrievals have also been rigorously compared to ground-based profiling radars in Antarctica, with CloudSat outperforming ERA-Interim grid-averaged results when MRR-derived retrievals are used as a reference dataset (Souverijns et al., 2018). Comparisons between CloudSat and existing reanalysis datasets are however scarce, and mostly limited to the Poles (Palerme et al., 2014, 2017; Milani et al., 2018; Behrangi et al., 2016). Together, these independent analyses provide confidence that CloudSat observations may deliver realistic accumulations on seasonal scales. The CloudSat snowfall dataset has also been proven useful for isolating distinct modes of snowfall variability on global scales. For instance, over-ocean convective snow has been comprehensively studied using CloudSat products (Kulie et al., 2016; Kulie and Milani, 2018). CloudSat also exhibits enhanced snowfall observational capabilities in mountainous regions compared to ground-based radar networks, partially due to scanning radar beam blockage issues (Smalley et al., 2014).

In spite of the noted shortcomings in snowfall datasets from gauge, radar and reanalyses, mountain snowfall has not yet been thoroughly studied using multiple reanalyses and the CloudSat data set. In this study, we derive mountain snowfall from five datasets (CloudSat 2CSP, MERRA, MERRA-2, ERA-Interim and JRA-55) to answer the following questions:

1. How much snow falls on the World's mountains?
2. What percentage of continental snow falls on mountainous regions?

Given the challenges in retrieving snowfall from single-frequency radar observations, especially in complex terrain, the CloudSat estimates are not treated as the "reference" dataset, though we note that they are the only estimates derived directly from observations. All five sources are treated as providing valid independent estimates of the fraction

https://doi.org/10.5194/tc-2019-302
Preprint. Discussion started: 4 February 2020


of snow that falls in mountainous regions to document the current state of knowledge in this field. The next section presents the different datasets employed in this study, as well as methodological information such as the mountain and continental masks. Section 3 compares mountain snowfall fraction and magnitudes between the different datasets while the following section, Section 4 discusses the differences in absolute magnitude of snowfall estimates. Finally, Section 5 summarizes the results of this study and offers concluding remarks.

## 2. Data and Methodology

### 2.1 Satellite observations

The nadir-pointing CPR onboard NASA's CloudSat satellite is the first spaceborne W-band (94-GHz) radar. CloudSat's high inclination orbit (98°) provides a unique coverage of observed global snowfall (Kulie et al., 2016). In addition to providing near-global sampling, the CPR has a minimum detectable radar reflectivity of approximately -29 dBZ and is consequently sensitive to lighter precipitation events (Tanelli et al., 2008). The CPR has a fixed field of view pointed at near-nadir and measures over a spatial resolution of approximately 1.7 km along-track and 1.4 km cross-track (Tanelli et al., 2008). The orbit is such that CloudSat revisits particular locations every 16 days. While this observing strategy limits sampling on short time-scales, CloudSat has observed more than 120 million snowing profiles over its 10+ year mission providing a rich dataset from which to derive snowfall frequency and cumulative snowfall over the large domains analyzed here.

CloudSat's 2CSP snowfall product, version R04 (Wood et al., 2013), provides estimates of instantaneous surface snowfall rates (S) for each of these pixels derived from the observed vertical profiles of radar reflectivity (Z). For this work, the data are spatially gridded onto a 1°x3° (lat/lon) grid to ensure robust sampling by the narrow CloudSat ground track. This means that the satellite data are sampled onto the spatial grid desired and then averaged within each grid. The product derives instantaneous data twice per month from an optimal estimation (Rodgers, 2000) retrieval applied to individual reflectivity profiles to obtain vertical profiles of snow microphysical properties. Ground clutter affects radar bins nearest the surface, so the retrieval is applied only to the clutter-free portion of the profile, i.e., that portion of the profile that is above the extent of likely ground clutter effects, typically about 1.2 km over land. Surface snowfall rate is estimated as the rate in the lowest clutter-free radar bin. The cumulative snowfall presented here are, thus, not true surface snowfall rates. Clutter also limits CloudSat's ability to detect shallow snow events or

https://doi.org/10.5194/tc-2019-302
Preprint. Discussion started: 4 February 2020


capture strong variations in snow profiles near the surface (Maahn et al, 2014; Souverijns et al, 2018; Palerme et al, 2017). While this introduces uncertainty in the snowfall estimates presented here, the analysis of ground-based vertically-pointing radar in mountainous regions by Maahn et al. (2014) show that the effects of this observing system limitations are somewhat compensated by the competing effects of evaporation and undetected shallow snowfall. It should also be noted that on November 1 2011, there was a change in CloudSat's operating mode, leading to daytime-only operations, which can lead to some uncertainty in the snowfall estimates.

Snow and rain are discriminated based on the CloudSat 2C-PRECIP-COLUMN product (Haynes et al., 2013), which applies a melting layer model driven by the ECMWF analyses temperature profiles. Snow particles are assumed to melt following the model of melted mass fraction described by Haynes et al. (2009). All profiles with melted fractions less than about 15% at the surface are considered snowing. Those with melted fractions greater than 90% are considered raining. Melted/frozen fractions between 15-90% are labeled "mixed" category considered to be a catch-all uncertainty for profiles that cannot be unambiguously classified as rain or snow using W-band reflectivity alone. Only snowing profiles are considered in this study.

### 2.2 Reanalyses

This study also considers four modern reanalyses: MERRA, MERRA-2, ERA-Interim and JRA-55. MERRA (Rienecker et al., 2011; 0.67° x 0.5° x 42 levels) uses the Goddard Earth Observing System version 5 (GEOS-5) and the data assimilation system (DAS). MERRA-2 (Gelaro et al., 2017; Bosilovich et al., 2015; 0.635° x 0.5° x 42 levels) was recently introduced to replace MERRA. ERA-Interim (Dee et al., 2011; 0.75° x 0.75° x 37 levels) is developed by the European Center for Medium Range Forecasts (ECMWF). ERA-Interim replaced the previous reanalysis dataset from the ECMWF, ERA-40. The Japanese Meteorological Agency (JMA) has recently developed their second reanalysis dataset after JRA-25: JRA-55 (Kobayashi et al., 2015; 0.56° x 0.56° x 60 levels). Both MERRA (Rienecker et al., 2011) and MERRA-2 (Gelaro et al., 2017) use 3D variational assimilation systems, where JRA-55 (Kobayashi et al., 2015) and ERA-Interim (Dee et al., 2011) use 4D. The spatial and temporal modeling of snowfall alone is different in these reanalyses, as are some of the physical mechanisms within. The MERRA-2 reanalysis assimilates an updated version of the GEOS-5 atmospheric model. Reichle et al. (2017) showed that the snow amounts are generally better represented in MERRA-2 than MERRA. However, MERRA-2 precipitation has a known deficiency

https://doi.org/10.5194/tc-2019-302
Preprint. Discussion started: 4 February 2020


over high topography due to issues in categorizing precipitation mode as large-scale instead of convective (Gelaro et al., 2017). The results from these previous studies make the comparison between MERRA and MERRA-2 particularly interesting in this case. JRA-55 assimilates the same observations that were used for the predecessor to ERA-Interim, ERA-40, as well as archived observations from JMA. Both JRA-55 and ERA-Interim use their own forecast models.

All datasets used in this study are bilinearly interpolated from their native resolution to match the 1°x3° (lat x lon) grid of CloudSat. The data are examined over the time period 2007-2016 with a monthly temporal resolution. The production of MERRA data ended in February 2016, as MERRA-2 is now the preferred dataset while CloudSat started in 2007.

### 2.3 Masks and definitions

Snowfall estimates from all sources are partitioned between the different continents using the "continental mask" shown in Figure 1a. The continental mask was first used in L'Ecuyer et al. (2015). Then, the mountain and non-mountain regions are separated using the "mountain mask" presented in Figure 1b. Based on the Kapos et al. (2000) definition, grid cells are classified as mountainous based on elevation, slope, and local elevation range. The original mask was produced using the USGS GTOPO30 digital elevation model, with a spatial resolution of 30 arc-seconds (~1 km). Our version of the mountain mask has been aggregated to 1°x3° (lat/lon) grid to match the spatial resolution of the gridded CloudSat 2SCP. The combination of these two masks is used to subdivide the snowfall estimates over the four continents that contain mountains: North America, South America, Eurasia and Africa.

In this article, total mountain snowfall is equal to the cumulative snow falling over North America, South America, Africa and Eurasia. Greenland and Antarctica are considered as ice sheets and therefore do not qualify as continents with mountains. Global snowfall is the cumulative snow falling over all lands in the world, which includes the four continents already cited plus Greenland, Australia and Antarctica.

## 3. Mountain snowfall estimates in CloudSat observations and reanalyses

### 3.1 Global spatial distribution of mountain snowfall

https://doi.org/10.5194/tc-2019-302
Preprint. Discussion started: 4 February 2020


Table 1 shows the snowfall estimates for mountain and non-mountain snowfall for CloudSat and the reanalyses, over each continent and globally. According to CloudSat observations, 1773 cubic km of snow falls over global mountains per year. This number is an average over the volume of snow falling during the time period from 2007 to 2016. From CloudSat estimates, 5% of global snowfall is within mountainous areas. To understand where the snow is falling, Figure 2a presents the geographical distribution of the mountain snowfall estimates in CloudSat. As expected, in all datasets a majority of the mountain snow falls in the Northern Hemisphere (Himalayas and Rockies; 95-99%), with little snowfall (<5%) in the Southern Hemisphere.

In the reanalyses, while the amount of snow falling over the mountains varies depending on the dataset examined, the fraction of snow within the mountains is similar across all datasets. MERRA and MERRA-2 global mountain snowfall estimates are close to CloudSat with 1763 cubic km per year and 1891 cubic km per year, respectively, while ERA-Interim and JRA-55 show much lower amounts, with 1041 cubic km per year and 489 cubic km per year, respectively. The systematically lower mountain snowfall estimates in ERA-Interim and in JRA-55, as well as the tendency for MERRA-2 to produce higher mountain snowfall rates over some continents will be further discussed below. In spite of these differences, the geographical distribution of mountain snowfall is similar between CloudSat and all the reanalyses (Fig. 2). It is encouraging that the fraction of snow falling in the mountains occupies a narrow range from 4% for MERRA's reanalyses and JRA-55 to 5 % for ERA-Interim and CloudSat. This good agreement between the different datasets (Table 1) allows us to state with some confidence that 5% of all continental snow falls in the mountains globally.

### 3.2 Contribution of mountain snowfall to continental snowfall

Table 1 also shows the contribution of mountain snowfall to total snowfall for CloudSat and each reanalysis over each continent. To get a better sense of the contribution of orography to snowfall, the percentage of mountainous grid points over each continent is provided in the last column of the table. Eurasia has the highest fraction of mountainous grid boxes with 33% of its grid boxes considered as mountains. North and South America have a quarter of their grid boxes covered with mountains and only 14% of the African continent is considered mountainous. The contribution of mountain snowfall does not vary substantially between continents. For Eurasia, South America and Africa, it is around 10 % while for North America it represents around 5% of the snow falling over the continent. Over

https://doi.org/10.5194/tc-2019-302
Preprint. Discussion started: 4 February 2020


all the continents, the agreement between the reanalyses and CloudSat observations is very good with differences under 4%.

Coherently with the previous section, the magnitude of mountain snowfall estimates over the four continents vary a lot depending on the datasets examined. MERRA's datasets and CloudSat present similar magnitude in terms of mountain and continental snowfall while ERA-Interim and JRA-55 present much lower estimates than the other datasets. For example, for mountain snowfall: over Eurasia the values for mountain snowfall vary between 379 for JRA-55 and 1440 cubic km per year for CloudSat. Over North America, it varies from 105 cubic km per year for JRA-55 to 378 cubic km per year for MERRA-2 and for South America from 5 for JRA-55 to 86 cubic km per year for MERRA-2. Unfortunately, the high range of differences observed for mountain snowfall also applies for the magnitude of total snowfall over each continent. In all cases, JRA-55 shows the lowest magnitude estimates and MERRA-2 the highest. It is also interesting to point out that CloudSat is always part of the higher range of snowfall estimates for each continent. Due to its limited temporal coverage, it might be missing some heavy snow events such as atmospheric rivers in Western North America (Rutz and Steenburgh, 2012; Lavers and Villarini, 2015; Molotch et al. 2010). These few events contribute to a large part of the water year precipitation.

## 4. Examination of the differences in snowfall magnitude

The previous section showed a very good agreement between all the datasets in terms of mountain snowfall fractions. However, the spatial maps presented in Figure 2 and the absolute snowfall amounts in Table 1 showed substantial differences in magnitude between the different datasets. This is further demonstrated in Figure 3 that summarizes the snowfall estimates in mm/month/grid box over Eurasia, North America, South America and Africa and its partitioning between mountainous (blue) and non-mountainous areas (yellow) for the five datasets. To ease the comparison between the different datasets, here the snowfall amounts are normalized by the number of mountain and non-mountain grid boxes respectively. There is some consistency in the relative behavior of the various datasets between the regions. Consistently with the results in Section 3, JRA-55 always has the lowest estimates of snowfall per grid box (cf. Table 1). For example, over North America and Eurasia, JRA-55 produces 68% less snowfall than the average of the four other datasets (Fig. 3). Even so, when looking at Figure 4, which presents the frequency of snowfall occurrences for each continent for all datasets, the frequency of snowfall occurrences for JRA-55 is very

https://doi.org/10.5194/tc-2019-302
Preprint. Discussion started: 4 February 2020


close to the other products. This indicates that JRA-55 underestimates the intensity of many snowfall events. ERA-Interim also tends to be on the lower end of the spectrum concerning snowfall, compared to the other datasets (Fig. 3). This can be at least partly attributed to its systematic lower frequency of snowfall occurrences (cf. Figure 4). With the exception of North America, MERRA-2 generally has the highest total snowfall compared to the other datasets (Fig. 3). Again, this is consistent with the results shown in the previous section. This overestimate is related to the way this dataset represents the frequency of snowfall events. MERRA-2 produces much more snowfall events than the other datasets (cf. Figure 4). This bias might be similar to the bias identified for precipitation in climate models, producing too frequent and too lightly-precipitating events, referred to as "perpetual drizzle" (Stephens et al., 2010). This could be happening for MERRA-2, for snowfall events.

The differences in snowfall among datasets is especially prominent over Africa and South America. Over Africa (Fig. 3d), both MERRA and MERRA-2 produce much more snow than the other datasets, with MERRA-2 producing nearly twice as much snowfall as MERRA. MERRA produces 75% more snowfall than the average of the three remaining datasets (ERA-Interim, JRA-55 and CloudSat) while for MERRA-2 produces 85% more. For the same reasons, over South America MERRA-2 produces 73% more snowfall than the average of the other datasets. Furthermore, it highly exceeds the mountain and non-mountain snowfall compared to the other datasets. However, as most of the snow over South America is mountainous, the excess in mountainous snowfall has a stronger impact on the differences in total accumulated snowfall. The seasonal cycle of mountain snowfall over South America (not shown) provides another interesting explanation for this specific bias. From January to December, MERRA-2 overestimates the other datasets but behave similarly, however during the second part of the cycle (after June), the behavior of MERRA-2 is very different. Instead of a decrease in mountain snowfall, snowfall accumulations remain very high and steady. This is clearly a major contributor to the high snowfall estimates of MERRA-2 over South America.

## 5. Summary and conclusion

Snowfall plays an important role in a number of atmospheric and surface processes that impact energy and hydrological cycles and can influence Earth's climate. To understand these processes, and how they will be influenced by future climate change, it is imperative to have reliable observations of present-day mountain snowfall. This study

https://doi.org/10.5194/tc-2019-302
Preprint. Discussion started: 4 February 2020


303 is a preliminary step towards an estimate of mountain snowfall from CloudSat satellite observations and four
304 reanalyses (MERRA, MERRA-2, JRA-55 and ERA-Interim). In this work we answer the following questions:
305 1. How much snow falls on the World's mountains?
306 1773 cubic km per year of snow falls on the World's mountains in CloudSat observations, 1763 cubic km per year in
307 MERRA, 1891 cubic km per year in MERRA-2, 1041 cubic km per year in ERA-Interim and 489 cubic km per year
308 in JRA-55 (cf. Table 1).
309 2. What percentage of continental snow falls on mountainous regions?
310 4 to 5% of snow falls over the mountains (cf. Table 1).
311
312 One aim of this research is to provide context for researchers for who want to use snowfall estimates globally
313 or on specific continents from reanalyses and/or satellite observations. The results of the discussion clearly emphasize
314 the necessity of using several datasets, including different platforms such as reanalyses and satellite observations.
315 Results presented here can help future analyses select validation datasets for specific continents, since we show that
316 some datasets behave differently than the others for continental snowfall estimates. For this reason, as well as the
317 acknowledgement by modelers that have difficulties accurately representing snowfall over South American mountains
318 (Gelaro et al., 2017), it is suspected that MERRA-2 is not the optimal dataset to use for this continent. However, this
319 study and Wrzesien et al. (2019) showed that over North America, MERRA-2 is certainly a realistic dataset with
320 substantial skills. Generally, there is no good or bad dataset, however some datasets may outperform others over
321 certain continents. These different abilities in the reanalyses and satellite products can lead to issues when validating
322 climate models, for example. It is therefore recommended to use an ensemble of the products just like it is
323 recommended to use several models or simulations. This study also suggests that estimates of the fraction of snow
324 that falls in the mountains may be more reliable than estimates of the absolute magnitude of mountain snow
325 accumulations. A hypothesis behind this result could be that the datasets presented here have a similar representation
326 of the large-scale forcings but differences at local/smaller scales, which could be due to uncertainties in the
327 microphysics. Indeed, even if the reanalyses are based on different models, they should simulate similar and realistic
328 large-scale forcings. For CloudSat, its ability to capture these forcings would come from its relatively good level of
329 temporal and spatial coverages. This could explain the consensus between the different datasets in terms of snowfall
330 fractions. On the other hand, at smaller scales, both types of datasets experience different limitations which would

https://doi.org/10.5194/tc-2019-302
Preprint. Discussion started: 4 February 2020


explain the dissimilarities in snowfall magnitude. For example for CloudSat, its spatial coverage could lead to miss some heavy snow events like atmospheric rivers.

In the future, this work will expand in several directions. First, a deeper and more process-oriented analysis of the differences observed during the different datasets should be done over each continent. While this study is confined to mountain snowfall produced by CloudSat and reanalysis datasets, it also serves as a foundation for studying cloud microphysical and dynamical processes operating within snow-producing clouds forced by orography. Because different modes of snowfall have varying impacts on the environment and potentially unique remote sensing fingerprints, identifying specific types of snowfall could lead to better measurements of snowfall. In addition, this could also improve forecasting by representing different snowfall modes more realistically within numerical weather models. Also, to evaluate the ability of climate models to represent snowfall estimates, this same analysis could be realized for climate models such as the CMIP5 ensemble, or the forthcoming CMIP6 ensemble.

**Acknowledgments and Data**

For ASD, this research was supported by a seed grant from the Center of Climatic Research of the University of Wisconsin-Madison. Parts of this work by TL was performed at the University of Wisconsin-Madison for the Jet Propulsion Laboratory, California Institute of Technology, sponsored by the National Aeronautics and Space Administration (NASA) CloudSat program. This work by MK was also partly supported by a NASA grant award NNX16AE21G. Parts of this research by NBW were performed at the University of Wisconsin - Madison for the Jet Propulsion Laboratory, California Institute of Technology, sponsored by the National Aeronautics and Space Administration. CloudSat data used herein were acquired from the CloudSat Data Processing Center (DPC) and at the time of writing can be accessed online at http://www.cloudsat.cira.colostate.edu; we acknowledge the support of the DPC in providing the data. MERRA and MERRA-2 data were provided by NASA's Global Modeling and Assimilation Office (GMAO) and obtained through the Goddard Earth Sciences Data and Information Services Center (GES DISC). JRA-55 data was provided by the Japanese Meteorological Agency and obtained through the National Center for Atmospheric Research's (NCAR) Research Data Archive. ERA-Interim data was provided by the European Centre for Medium-Range Weather Forecasts (ECMWF) and obtained via the ECMWF WebAPI.

https://doi.org/10.5194/tc-2019-302
Preprint. Discussion started: 4 February 2020




359 **References**

360 Barnett, T. P., Adam, J. C., and Lettenmaier, D. P.: Potential impacts of a warming climate on water
361 availability in snow-dominated regions. Nature, 438(7066), 303–309. http://doi.org/10.1038/nature04141, 2005.
362 Behrangi, A., M. Christensen, M. Richardson, M. Lebsock, G. Stephens, G. J. Huffman, D. Bolvin, R. F.
363 Adler, A. Gardner, B. Lambrigtsen, and E. Fetzer: Status of high-latitude precipitation estimates from observations
364 and reanalyses, J. Geophys. Res. Atmos., 121, 4468-4486, doi: 10.1002/2015JD024546, 2016.
365 Bosilovich, M.G., J. Chern, D. Mocko, F.R. Robertson, and A.M. da Silva: Evaluating Observation Influence
366 on Regional Water Budgets in Reanalyses. J. Climate, 28, 3631–3649, https://doi.org/10.1175/JCLI-D-14-00623.1,
367 2015.
368 Bromwich, D. H., J. P. Nicolas, and A. J. Monaghan: An assessment of precipitation changes over Antarctica
369 and the Southern Ocean since 1989 in contemporary global reanalyses, J. Clim., 24, 4189-4209,
370 doi:10.1175/2011JCLI4074.1, 2011.
371 Cao, Q, Y. Hong, S. Chen, J.J. Gourley, J. Zhang and P.E. Kirstetter: Snowfall Detectability of NASA'S
372 CloudSat: The first cross-investigation of its 2C-Snow-Profile Product and National Multi-sensor Mosaic QPE (NMQ)
373 Snowfall Data. Progress in Electromagnetics Research, Vol. 148, 55-61, 2014.
374 Chen, T., J. Guo, Z. Li, C. Zhao, H. Liu, M. Cribb, F. Wang, and J. He: A CloudSat Perspective on the Cloud
375 Climatology and Its Association with Aerosol Perturbations in the Vertical over Eastern China. J. Atmos. Sci., 73,
376 3599–3616, https://doi.org/10.1175/JAS-D-15-0309.1, 2016.
377 Daloz, A.S., E. Nelson, T. L'Ecuyer, A.D. Rapp, and L. Sun. Assessing the Coupled Influences of Clouds on
378 the Atmospheric Energy and Water Cycles in Reanalyses with A-Train Observations. J. Climate, 31, 8241–8264,
379 https://doi.org/10.1175/JCLI-D-17-0862.1, 2018.
380 Dee, D. P., and co-authors: The ERA-Interim reanalysis: configuration and performance of the data
381 assimilation system, Quart. J. Roy. Meteor. Soc., 137, 553-597, doi: 10.1002/qj.828, 2011.
382 Gelaro, R., and co-authors: The Modern-Era Retrospective Analysis for Research and Applications, Version
383 2 (MERRA-2), J. Climate, 30, 5419-5454, doi: 10.1175/JCLI-D-16-0758.1, 2017.
384 Goodison B., P.Y.T. Louie and D. Yang: WMO solid precipitation measurement intercomparison : Final
385 report. WMO/TD No. 872. WMO, Geneva 88pp. plus annexes 212pp, 1998.

https://doi.org/10.5194/tc-2019-302
Preprint. Discussion started: 4 February 2020




386 Groisman, P. Y., and D. R. Legates: The accuracy of United States precipitation data. Bull. Am. Meteorol.
387 Soc., 75, 215-227, 1994.
388 Guan, B., Molotch, N. P., Waliser, D. E., Fetzer, E. J., and Neiman, P. J.: Extreme snowfall events linked to
389 atmospheric rivers and surface air temperature via satellite measurements, Geophys. Res. Lett., 37, L20401,
390 doi:10.1029/2010GL044696, 2010.
391 Haynes, J. M., T. S. L'Ecuyer, G. L. Stephens, S. D. Miller, C. Mitrescu, N. B. Wood, and S. Tanelli, 2009:
392 Rainfall retrieval over the ocean with spaceborne W-band radar. J. Geophys. Res., 114, D00A22,
393 doi:10.1029/2008JD009973.
394 Haynes, J. M., and co-authors: Level 2-C Precipitation Column algorithm product process description and
395 interface control document, version P2_R04. CloudSat Project technical document, National Aeronautics and Space
396 Administration, 17 pp. Available from http://www.cloudsat.cira.colostate.edu/sites/default/files/products/files/2C-
397 PRECIP-COLUMN_PDICD.P2_R04.20130124.pdf, last access 20 June 2019, 2013..
398 Henn, B., Newman, A. J., Ben Livneh, Daly, C., & Lundquist, J. D.: An assessment of differences in gridded
399 precipitation datasets in complex terrain. Journal of Hydrology, 556, 1205–1219.
400 http://doi.org/10.1016/j.jhydrol.2017.03.008, 2018.
401 Hiley, M.J., M.S. Kulie, and R. Bennartz: Uncertainty Analysis for CloudSat Snowfall Retrievals. J. Appl.
402 Meteor. Climatol., 50, 399–418, https://doi.org/10.1175/2010JAMC2505.1, 2011.
403 Kapos, V., J.Rhind, M. Edwards, M.F. Price and C. Ravilious: Developing a map of the world's mountain
404 forests. In: Forests in Sustainable Mountain Development: A State-of-Knowledge Report for 2000, M.F. Price and N.
405 Butt (eds.), CAB International, Wallingford: 4–9, 2000.
406 Kidd, C., A. Becker, G.J. Huffman, C.L. Muller, P. Joe, G. Skofronick-Jackson, and D.B. Kirschbaum: So,
407 How Much of the Earth's Surface Is Covered by Rain Gauges?. Bull. Amer. Meteor. Soc., 98, 69–78,
408 https://doi.org/10.1175/BAMS-D-14-00283.1, 2017.
409 Kobayashi, S., and Coauthors: The JRA-55 Reanalysis: General Specifications and Basic Characteristics, J.
410 Meteor. Soc. Japan, 93, 5-48, doi: 10.2151/jmsj.2015-001, 2015.
411 Kochendorfer J. and Co-authors: Testing and development of transfer functions for weighing precipitation
412 gauges in WMO-SPICE. Hydrol. Earth. Syst. Sc., 22, 1437-1452, doi:10.5194/hess-22-1437-2018, 2018.

https://doi.org/10.5194/tc-2019-302
Preprint. Discussion started: 4 February 2020




413 Kulie, M. S., and R. Bennartz: Utilizing spaceborne radars to retrieve dry snowfall. J. Appl. Meteorol. Clim.
414 48, 2564-2580, 2009.
415 Kulie, M.S., L. Milani, N.B. Wood, S.A. Tushaus, R. Bennartz, and T.S. L'Ecuyer: A Shallow Cumuliform
416 Snowfall Census Using Spaceborne Radar. J. Hydrometeor., 17, 1261–1279, https://doi.org/10.1175/JHM-D-15-
417 0123.1, 2016.
418 Kulie, MS, Milani, L. Seasonal variability of shallow cumuliform snowfall: A Cloud-Sat perspective. Q J R
419 Meteorol Soc; 144 ( Suppl. 1): 329– 343. https://doi.org/10.1002/qj.3222, 2018.
420 Lavers, D.A., and G. Villarini: The contribution of atmospheric rivers to precipitation in Europe and the
421 United States, Journal of Hydrology, Volume 522, Pages 382-390, ISSN 0022-1694,
422 https://doi.org/10.1016/j.jhydrol.2014.12.010, 2015.
423 L'Ecuyer, T.S., H.K. Beaudoing, M. Rodell, W. Olson, B. Lin, S. Kato, C.A. Clayson, E. Wood, J. Sheffield,
424 R. Adler, G. Huffman, M. Bosilovich, G. Gu, F. Robertson, P.R. Houser, D. Chambers, J.S. Famiglietti, E. Fetzer,
425 W.T. Liu, X. Gao, C.A. Schlosser, E. Clark, D.P. Lettenmaier, and K. Hilburn: The Observed State of the Energy
426 Budget in the Early Twenty-First Century. J. Climate, 28, 8319–8346, https://doi.org/10.1175/JCLI-D-14-00556.1,
427 2015.
428 Liu, G.: Deriving snow cloud characteristics from CloudSat observations. J. Geophys. Res., 113, D00A09,
429 doi:10.1029/2007JD009766, 2008.
430 Maahn, M., C. Burgard, S. Crewell, I. V. Gorodetskaya, S. Kneifel, S. Lhermitte, K. Van Tricht, and N. P.
431 M. van Lipzig: How well does the spaceborne radar blind zone affect derived surface snowfall statistics in polar
432 regions?, J. Geophys. Res. Atmos., 119, 132604-132620, doi: 10.1002/2014JD022079, 2014.
433 Mankin, J.S., D. Viviroli, D. Singh, A.Y. Hoekstra, and N.S. Diffenbaugh: The potential for snow to supply
434 human water demand in the present and future. Environ. Res. Lett., 10, no. 11, 114016, doi:10.1088/1748-
435 9326/10/11/114016, 2015.
436 Neiman, P. J., F. M. Ralph, G. A. Wick, J. D. Lundquist, and M. D. Dettinger: Meteorological characteristics
437 and overland precipitation impacts of atmospheric rivers affecting the west coast of North America based on eight
438 years of SSM/I satellite observations. J. Hydrometeor., 9, 22–47, 2008.

https://doi.org/10.5194/tc-2019-302
Preprint. Discussion started: 4 February 2020




Milani, L., and co-authors: CloudSat snowfall estimates over Antarctica and the Southern Ocean: An assessment of independent retrieval methodologies and multi-year snowfall analysis. Atmospheric Research 213, DOI:10.1016/j.atmosres.2018.05.015, 2018.

Norin, L., Devasthale, A., L'Ecuyer, T. S., Wood, N. B., and Smalley, M.: Intercomparison of snowfall estimates derived from the CloudSat Cloud Profiling Radar and the ground-based weather radar network over Sweden, Atmos. Meas. Tech., 8, 5009-5021, https://doi.org/10.5194/amt-8-5009-2015, 2015.

Palerme, C., C. Claud, A. Dufour, C. Genthon, N. B. Wood, and T. L'Ecuyer: Evaluation of Antarctic snowfall in global meteorological reanalyses, Atmos. Res., 190, 104-112, doi: 10.1016/j.atmosres.2017.02.015, 2017.

Palerme, C., J. E. Kay, C. Genthon, T. L'Ecuyer, N. B. Wood, and C. Claud: How much snow falls on the Antarctic ice sheet?, The Cryosphere, 8, 1577-1587, doi: 10.5194/tc-8-1577-2014, 2014.

Ralph, F. M., P. J. Neiman, G. A. Wick, S. I. Gutman, M. D. Dettinger, D. R. Cayan, and A. B. White: Flooding on California's Russian River: Role of atmospheric river. Geophys. Res. Lett., 33, L13801, doi:10.1029/2006GL026689, 2006.

Reichle, R.H., Q. Liu, R.D. Koster, C.S. Draper, S.P. Mahanama, and G.S. Partyka: Land Surface Precipitation in MERRA-2. J. Climate, 30, 1643–1664, https://doi.org/10.1175/JCLI-D-16-0570.1, 2017.

Rienecker, M. M., and Coauthors: MERRA: NASA's Modern-Era Retrospective Analysis for Research and Applications, J. Climate, 24, 3624-3648, doi: 10.1175/JCLI-D-11-00015.1, 2011.

Rodell, M., J.S. Famiglietti, D. N. Wiese, J.T. Reager, H.K. Beaudoing, F.W., Landerer and M.-H. Lo, 2018: Emerging trends in global freshwater availability. Nature 557, 651-659.

Rodgers, C. D.: Inverse Methods for Atmospheric Sounding: Theory and Practice. Series on Atmospheric and Oceanic and Planetary Physics, Vol. 2, World Scientific, 256, 2000.

Rutz, J. J. and Steenburgh, W. J.: Quantifying the role of atmospheric rivers in the interior western United States. Atmosph. Sci. Lett., 13: 257-261. doi:10.1002/asl.392, 2012.

Smalley, M., L'Ecuyer, T., Lebsock, M., and Haynes, J.: A comparison of precipitation occurrence from the NCEP Stage IV QPE product and the CloudSat cloud profiling radar, J. Hydrometeorol., 15, 444– 458, doi:10.1175/JHM-D-13-048.1, 2014.

Smalley, M. and T. S. L'Ecuyer: A global assessment of the spatial scale of precipitation occurrence. J. Appl. Meteor. and Climatol., 54, 2179-2197, 2015.

https://doi.org/10.5194/tc-2019-302
Preprint. Discussion started: 4 February 2020


Souverijns, N., Gossart, A., Lhermitte, S., Gorodetskaya, I. V., Grazioli, J., Berne, A., Duran-Alarcon, C., Boudevillain, B., Genthon, C., Scarchilli, C., and van Lipzig, N. P. M.: Evaluation of the CloudSat surface snowfall product over Antarctica using ground-based precipitation radars, The Cryosphere, 12, 3775-3789, https://doi.org/10.5194/tc-12-3775-2018, 2018.

Stephens, G. L., and Coauthors: The CloudSat mission and the A-Train, Bull. Amer. Meteor. Soc., 83, 1771-1790, doi: 10.1175/BAMS-83-12-1771, 2002.

Stephens, G. L., and co-authors: CloudSat mission: Performance and early science after the first year of operation. J. Geophys. Res., 113, D00A18, doi:10.1029/2008JD009982, 2008.

Stephens and co-authors: Dreary state of precipitation in global models, Journal for Geophysical Research, 115,D24211, doi:10.1029/2010JD014532, 2010.

Tanelli, S., S. L. Durden, E. Im, K. S. Pak, D. G. Reinke, P. Partain, J. M. Haynes, and R. T. Marchand: CloudSat's Cloud Profiling Radar after two years in orbit: Performance, calibration, and processing, IEEE Trans. Geosci. Remote Sens., 46, 3560-3573, doi: 10.1109/TGRS.2008.2002030, 2008.

Viale, M. and M.N. Nuñez: Climatology of Winter Orographic Precipitation over the Subtropical Central Andes and Associated Synoptic and Regional Characteristics. J. Hydrometeor., 12, 481–507, https://doi.org/10.1175/2010JHM1284.1, 2011.

Wood, N., T. L'Ecuyer,, D. Vane,, G. Stephens,, and P. Partain: Level 2C Snow Profile Process Description and Interface Control Document, Algorithm Version P_R04. NASA JPL CloudSat project technical document revision 0, 21 pp. Available from http://www.cloudsat.cira.colostate.edu/sites/default/files/products/files/2C-SNOW-PROFILE_PDICD.P_ R04.20130210.pdf, last access 3 August 2015, 2013.

Wood, N. B., and T. S. L'Ecuyer: Level 2C Snow Profile Process Description and Interface Control Document, Product Version P1_R05. NASA JPL CloudSat project document revision 0., 26 pp. Available from http://www.cloudsat.cira.colostate.edu/sites/default/files/products/files/2C-SNOW-PROFILE_PDICD.P1_R05.rev0_.pdf, last access 20 June 2019, 2018.

Wrzesien, M. L., Durand, M. T., and Pavelsky, T. M: A reassessment of North American River basin cool-season precipitation: Developments from a new mountain climatology data set. Water Resources Research, 55. https://doi.org/10.1029/2018WR024106, 2019.

https://doi.org/10.5194/tc-2019-302
Preprint. Discussion started: 4 February 2020




**Tables**

| Snowfall estimates | MERRA | MERRA-2 | ERA-Interim | JRA-55 | CloudSat | Percentage of mountain grid boxes per continent |
|---|---|---|---|---|---|---|
| **Eurasia** | 1416 /11176 **11%** | 1426 / 13104 **10%** | 808 /8112 **9%** | 379 / 3916 **9%** | 1440 / 10764 **12%** | 33% |
| **North America** | 312 / 4500 **6%** | 378/5800 **6%** | 223 /3450 **6%** | 105 / 1725 **6%** | 303 / 7325 **4%** | 24% |
| **South America** | 30 / 270 **10%** | 86 / 662 **12%** | 10 / 100 **9%** | 5 / 46 **10%** | 30 / 236 **11%** | 21% |
| **Africa** | 0.5 / 6 **8%** | 0.8 / 11 **7%** | 0.1 / 1 **9%** | 0.07 / 0.5 **12%** | 0.2 / 2 **9%** | 14% |
| **Global** | 1763/ 43403 **4%** | 1891/47127 **4%** | 1041/21363 **5%** | 489/11288 **4%** | 1773/35027 **5%** | |

**Table 1:** The table summarizes the snowfall estimates of mountain and non-mountain snowfall for MERRA, MERRA-2, ERA-Interim, JRA-55 and CloudSat for the time period 2007-2016, for Eurasia, North America, South America, Africa and globally. For each area and dataset, a table cell shows: the amount of mountain (top left), non-mountain snow (top right; cubic km per year) and the contribution of mountain snow to the total amount of snow falling over a continent (bottom, %). The last column shows the percentage of grid boxes considered as mountain by the mountain mask over each continent.

**Figures**

https://doi.org/10.5194/tc-2019-302
Preprint. Discussion started: 4 February 2020




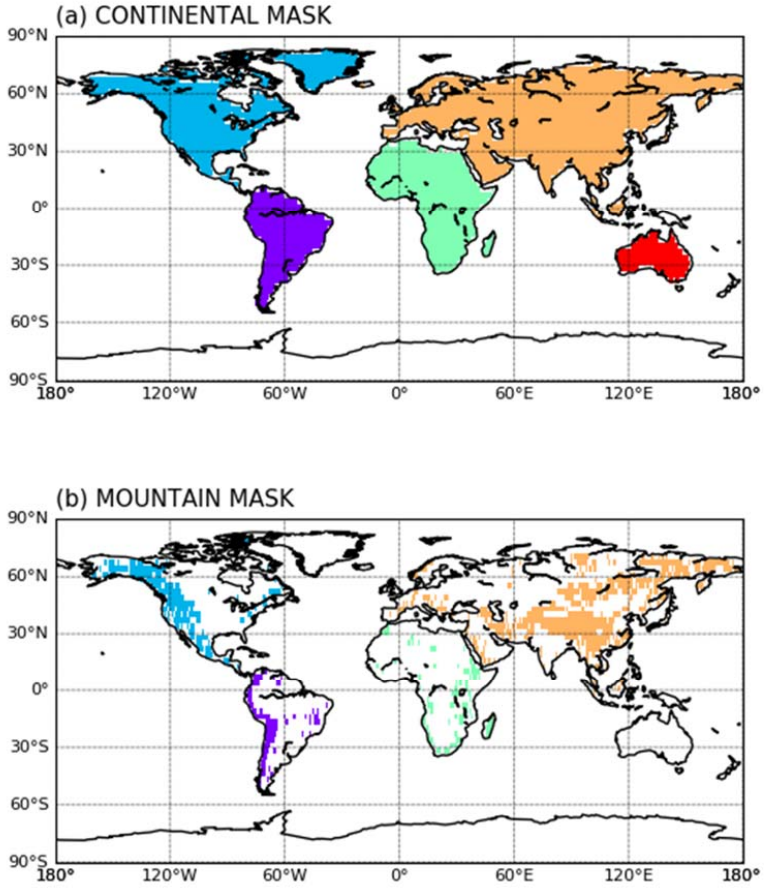


511
512
513
514 **Figure 1:** Spatial maps of the continental mask (a) with specific colors for each continent: blue for North America,
515 pink for South America, orange for Eurasia, green for Africa, red for Australia and white for Antarctica; and the
516 associated mountain mask (b) for each continent containing mountains.
517

https://doi.org/10.5194/tc-2019-302
Preprint. Discussion started: 4 February 2020




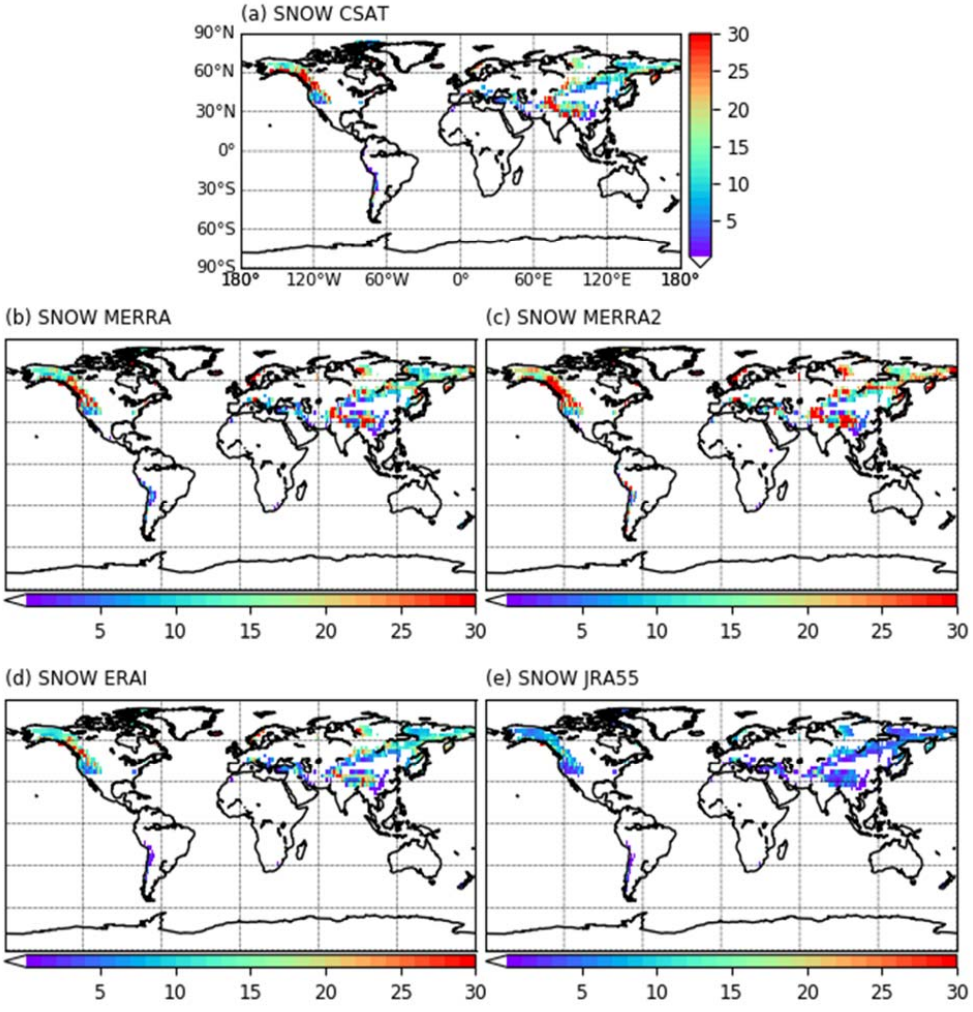


**Figure 2:** Spatial maps of global cumulative mountain snowfall (mm/month/gridbox) for a) CloudSat, b) MERRA, c) MERRA-2, d) ERA-Interim and d) JRA-55, averaged over the time period 2007-2016.

https://doi.org/10.5194/tc-2019-302
Preprint. Discussion started: 4 February 2020


The Cryosphere
Discussions
Open Access
EGU

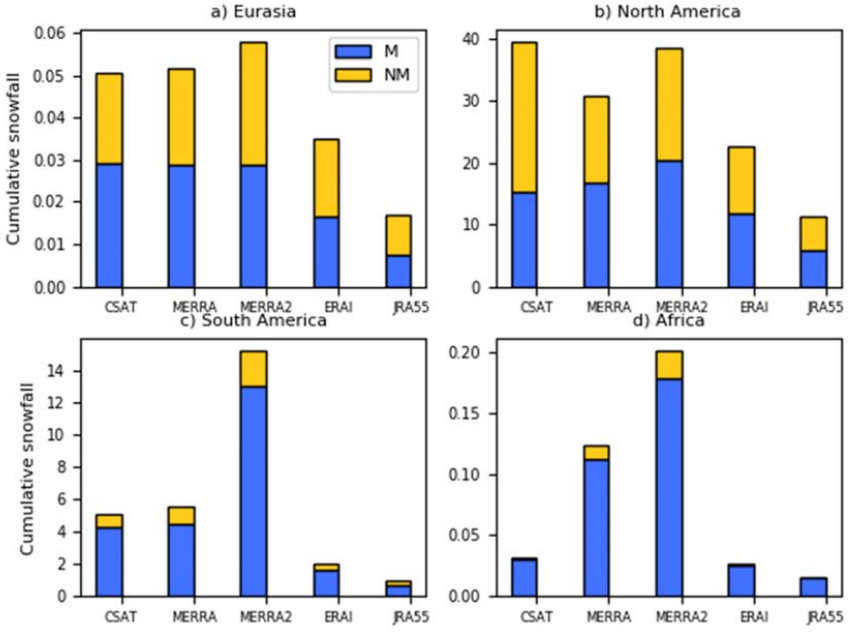


**Figure 3:** Snowfall estimates (mm/month/grid box) over: a) Eurasia, b) North America, c) South America and d) Africa for CloudSat, MERRA, MERRA-2, ERA-Interim and JRA-55 over the time period 2007-2016. Mountain snow is in blue and non-mountain snow is in yellow.

https://doi.org/10.5194/tc-2019-302
Preprint. Discussion started: 4 February 2020


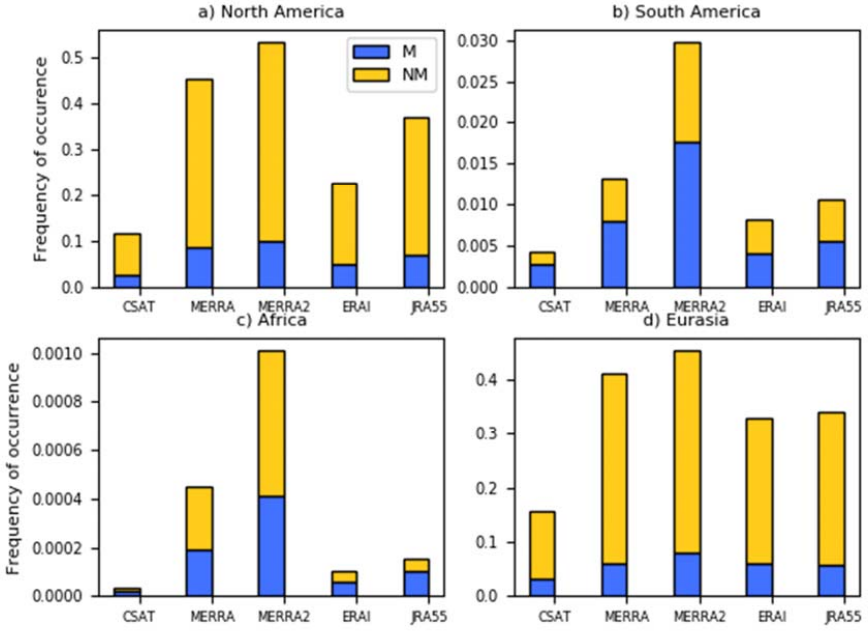


**Figure 4:** Frequency of occurrence of snowfall estimates over: a) Eurasia, b) North America, c) South America and d) Africa for CloudSat, MERRA, MERRA-2, ERA-Interim and JRA-55 over the time period 2007-2016. Mountain snow is in blue and non-mountain snow is in yellow.